

---

# Microfabrication Methods for Miniature Heat Engines

---

## Personnel

A. Ayon, R. A. Braff, D.-Z. Chen, R. Ghodssi, and C.-C. Lin  
(M. A. Schmidt in collaboration with Microengine Team)

## Sponsorship

ARO and DARPA

As part of the microturbine engine activity at MIT, we are developing novel process technologies for fabrication of these devices. These processes define the state-of-art in two important MEMS technologies: aligned wafer bonding and Deep Reactive Ion Etching (DRIE). We have recently completed a full matrix experiment for characterization of the deep reactive ion etch process. This experiment has resulted in a set of parameters which permits design of etch processes to specific needs of etch rate, anisotropy, aspect ratio dependent etching,

and uniformity. We have been successful in applying this to a variety of etched structures. The aligned wafer bonding is needed to create laminations of many individually etched wafers in order to create 3-D structures. We have already achieved 5 layers of aligned wafer bonds for a micro-bearing test rig. Finally, this program is providing process support for an ensemble of fabricated structures in the microturbine program, as illustrated in Figure 1. □

*Fig. 1: Fabrication challenges in a microturbine engine. (Courtesy of Prof. Epstein)*

# Micro Motors and Generators for Micro Turbomachinery

## Personnel

S. F. Nagle, L. Frechette, R. Ghodssi, and A. Ayon  
(J. H. Lang, S. D. Senturia, S. D. Umans, and E. P. Warren in collaboration with K. S. Breuer, F. E. Ehrich, A. H. Epstein, S. Jacobsen, M. S. Spearing, C. S. Tan, I. A. Waitz, and R. Walker)

## Sponsorship

ARO and DARPA

This project is part of the MIT Micro Gas Turbine Engine Project. The MIT Micro Gas Turbine Engine Project has the ambitious goal of using MEMS fabrication technologies to construct compact electric power generation systems from a gas turbine generator comprising a compressor, combustor, turbine and electric generator. Other systems under development include separate motor/compressors and turbine/generators. The MIT Micro Gas Turbine Engine Project is highly interdisciplinary, involving students, staff and faculty from several academic departments and laboratories.

This project seeks to develop the motors and generators employed in the micro turbomachines mentioned above, and to develop their power and control electronics. Following the analysis of several candidates, we have selected the electric induction machine for these applications. Our electric machine is disk-shaped, and is shown in edge view in Figure 2. On one side of its air gap, stator electrodes are supported by an insulator deposited on a substrate. They are connected to form one or more phases, and are used to impose a potential wave which travels around the stator. On the other side of the air gap is the rotor, which rotates as a disk. The rotor consists of a conducting film supported by an insulator deposited on a substrate.

During motoring operation, the power electronics excite the stator electrodes to produce a potential wave which travels around the stator with a speed exceeding that of the rotor. This wave, and the corresponding charges which reside on the stator electrodes, induce image charges on the rotor surface across the air gap. Since the speed of the traveling potential wave exceeds the mechanical speed of the rotor, convection alone can not synchronize the rotor charges with the traveling wave, as must happen in steady state. Thus, the rotor charges must conduct through the rotor film to maintain synchronism. The conduction process must in turn be driven by a tangential electric field, and so the rotor charges lag behind the potential wave to produce that field, as shown in Figure 2. Finally, the tangential electric field acts on the rotor charges to impart a tangential surface stress on the rotor, which in turn results in a motoring torque. During generating operation, the rotor speed exceeds that of the traveling potential wave, and the torque is reversed.

To date, we have derived detailed dynamic models of the electric induction machine, and have used those models to develop an optimized 6-phase machine having a 4-mm diameter. As a motor, we expect this machine to

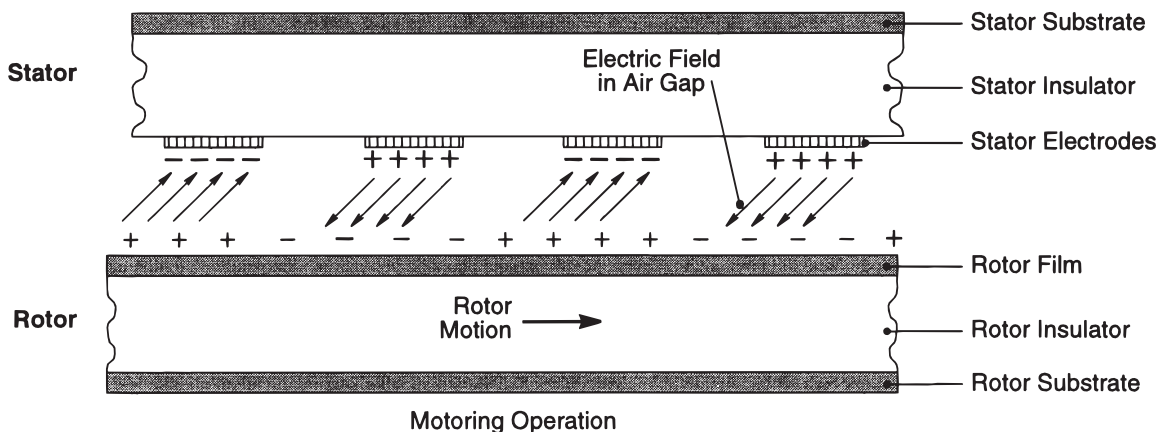


Fig. 2: Edge view of the electric induction machine.

*continued*

---

## Vibration-to-Electric Energy Conversion

---

### Personnel

J. O. Mur-Miranda and R. Amirtharajah  
(J. H. Lang and A. P. Chandrakasan)

### Sponsorship

Draper Laboratory

produce a 3-W mechanical output at 2.4 Mrpm when its phases are excited with 300-V 3-MHz sinusoids. To support this design effort, we have characterized the conductivity of its polysilicon rotor film, the electrical breakdown of the air gaps between its stator electrodes, and the physical properties of the thick silicon dioxide films to be used as its rotor and stator insulators. Finally, we have designed, fabricated and demonstrated control electronics and resonant power electronics to support motoring operation. Our work now focuses on the fabrication and testing of several experimental motors including a tethered motor and a motor/compressor. A drawing of the tethered motor is shown in Figure 3. In this motor, the rotor is stationary, and is supported by mechanical tethers, or springs. The bending of the tethers will be used to accurately measure torque. □

We are developing a method for converting ambient vibration energy into electric energy for general purpose consumption. Such energy conversion is useful for powering autonomous electronics such as remote sensors.

Our method has two key components which are under development as an integrated system. The first component is a MEMS structure comprising a proof mass, its suspension and a variable capacitor. The capacitor is the actual energy converter. The second component is the combined power and control electronics for the system. These electronics are under design following the paradigm of very-low-power electronics since their power consumption is a tax on the converted energy.

The project goals for this year are to develop models for the system, and to optimize the system design to maximize output power per system area. A bearing-vibration-monitoring application serves to guide the design optimization. These goals have essentially been met, and the fabrication and testing of several energy converters is expected to begin soon. □

Fig. 3: Perspective view of the tethered electric induction motor.

# Development of a Hydrogen Combustor for a Microfabricated Gas Turbine Engine

## Personnel

A. Mehra and I. A. Waitz

## Sponsorship

Gas Turbine Laboratory, Department of Aeronautics and Astronautics

As part of the MIT micro engine program to develop a micro gas turbine engine capable of producing 50W of electrical power in a package less than one cubic centimeter in volume, we have completed the fabrication and testing of the first-ever hydrogen combustor micromachined from silicon. Complete with a fuel manifold and injector holes, the combustion chamber measuring less than 70 mm<sup>3</sup> in volume has been successfully demonstrated to provide exit temperatures up to 1800K. The combustor has been experimentally tested at elevated pressures and temperatures for over fifteen hours, thereby demonstrating the satisfactory performance of silicon in such environments.

The micro-fabricated combustor consists of a stack of three fusion-bonded silicon wafers (Figure 4). Double-sided photolithography was used on all three wafers to pattern the fuel manifold, injectors, combustion chamber and fluid flow paths. Deep Reactive-Ion Etching (DRIE), employing a time multiplexed inductively coupled plasma of SF<sub>6</sub> and C<sub>4</sub>F<sub>8</sub>, was used to etch deep cavities and high aspect ratio anisotropic structures (Figure 5a).

The combustion chamber was isotropically dry-etched from a single 1000m wafer (Figure 5b). The complete device required five masks and six deep etches. An additional four-mask process has already been designed to include compressor and turbine stator vanes, "on-chip" spark and resistive igniters, and a resistive wall temperature sensor for engine feedback control.

Experimental test results for the micro-combustor demonstrated peak exit temperatures of 1800K, with relatively cooler walls at 1000K (Figure 6). The combustor efficiency however, was found to be between 40%-60%, due to high heat loss resulting from a large surface area-to-volume ratio in the micro-device. While the performance of silicon was found to be creep limited at excessively high temperatures and pressures, the microcombustor and turbine stator vanes have been successfully tested for several hours at operating conditions sufficient to complete a micro-gas turbine cycle. These results are the first step towards establishing the viability of building a new generation of high-energy density micro-devices using silicon microfabrication techniques.

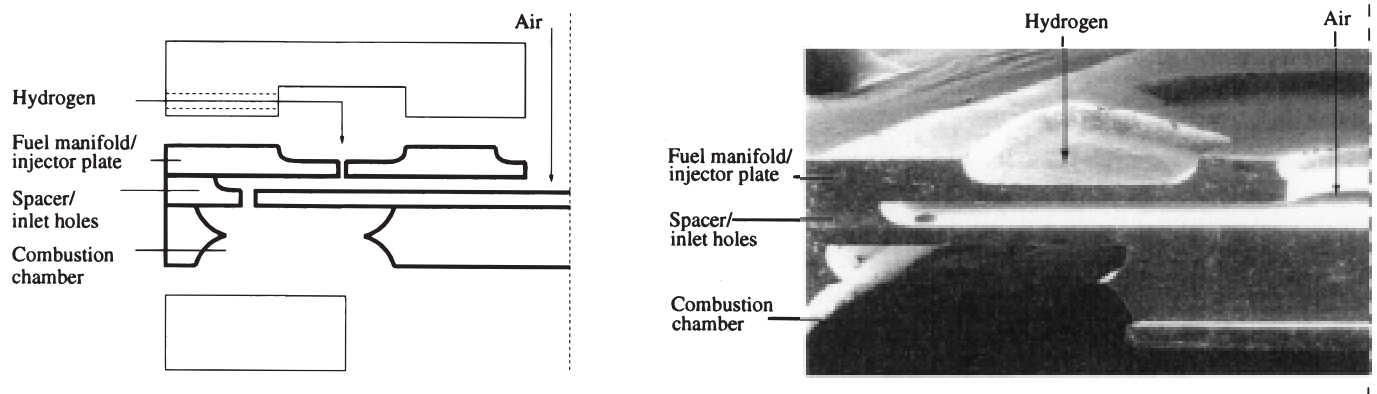


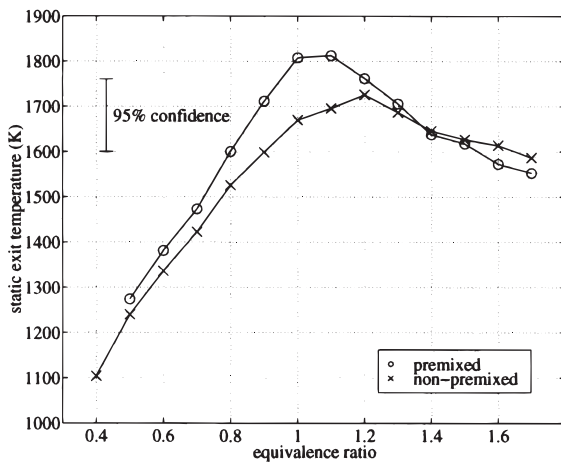
Fig. 4: Schematic and SEM cross-section of the combustor showing the fuel manifold, injector holes, and air flow path through the combustor.

*continued*

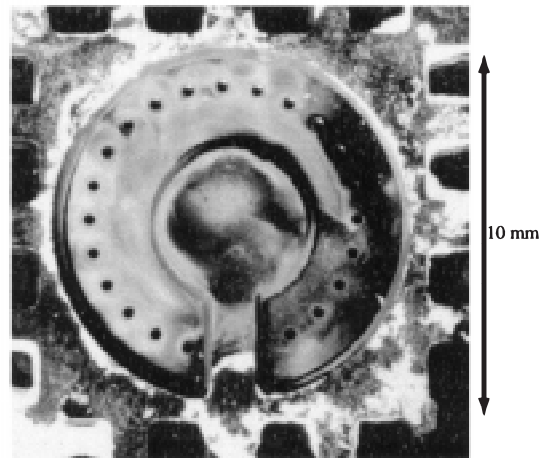
continued

The first public report of this work will be presented at the Hilton Head Solid-State Sensor and Actuator Workshop in June 1998. □

Fig. 5: SEM's of the fuel manifold and combustion chamber.



(a) Microcombustor test results, showing exit temperatures up to 1800K



(b) Post-combustion appearance of the rig after 15 hours of testing at  $T_{exit} \sim 1600K$

Fig. 6: Experimental test results for the microcombustor.

---

# DRIE-Fabricated Nozzles for Generating Supersonic Flows in Micropropulsion Systems

---

## Personnel

R. L. Bayt  
(K. S. Breuer)

## Sponsorship

NASA/JPL

Various trends in the spacecraft industry are driving the development of low-thrust propulsion systems. These may be needed for fine attitude control, or to reduce the mass of the propulsion system through the use of small lightweight components. The nozzle converts the stored energy in the pressurized gas into kinetic energy through an expansion. The nozzle efficiency is characterized by the amount of kinetic energy leaving the nozzle, and is governed by the exit Mach number. Due to the increase in viscous losses as scale is reduced, it was feared that supersonic flows could not be generated in microdevices. However, flow modeling reveals that the reduction in scale can be offset by an increase in operating pressure to maintain a constant Reynolds number. Therefore, thrust can be decreased by reducing the nozzle scale, and viscous losses are mitigated by running at higher chamber pressures.

In order to operate a supersonic nozzle efficiently, the geometry must be contoured to guard against flow separation. Deep Reactive Ion Etching enables extruded flow channels of arbitrary in-plane geometry to be created at scales an order of magnitude smaller than conventional machining. These channels are encapsulated by anodically bonding Pyrex to the upper and lower surfaces. Testing indicates that 11.3 milliNewtons of thrust is generated for a nozzle with a  $37\ \mu\text{m}$  throat width and a 17.1 exit to throat area ratio. The exit velocity was 590 m/s, which corresponds to an exit Mach number of 3.8. This is 50 m/s higher than previously achieved in a micromachined device and demonstrates that supersonic flows can be generated at this scale. Future work will focus on further improvements to the flow model as well as evaluating methods for enhancing the performance of the nozzle by heating the flow. □

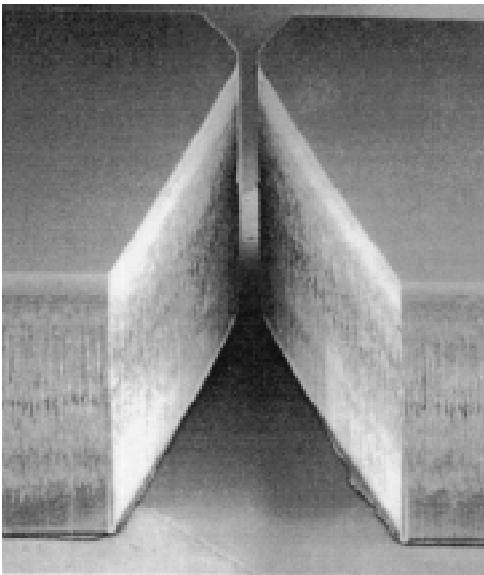


*Fig. 7: DRIE etched nozzle with a  $19\ \mu\text{m}$  throat width and  $308\ \mu\text{m}$  deep. Upper and lower surfaces are anodically bonded to Pyrex to enclose the flow channel and allow gas to be discharged out of the page.*

---

## Gas Film Lubrication in High Speed MEMS devices

---

### Personnel

D. J. Orr, E. S. Piekos, and C. C. Lin  
(K. S. Breuer)

### Sponsorship

ARO and DARPA

As part of the MIT Microengine project, we are investigating the issues associated with the design and analysis of low drag, high-performance gas film lubrication systems for use in high speed rotating MEMS devices. The microengine requires lubrication of components rotating at speeds in excess of 2 million RPM with clearances as small as one micron. We are studying effects of fabrication tolerances, materials and operating conditions on the performance of such lubrication devices.

The tools developed for this include high-accuracy numerical simulation tools to study the steady and unsteady motion of MEMS journal bearings, a scaled-up test rig (26x full scale) and a full-scale micro-bearing test rig - a bearing test facility fabricated using advanced MEMS techniques. Issues of interest are the extent to which we can rely on conventional analysis tools (such as the Reynolds lubrication equations), the rotor dynamics of MEMS bearings and instrumentation issues for high-speed MEMS devices. □

---

## Microelectromechanical Test Structures (M-Test)

---

### Personnel

R. Gupta and E. Deutsch  
(S. D. Senturia in collaboration with the research groups of M. Schmidt and C. Thompson)

### Sponsorship

SRC and DARPA

The goal of this project is the development of a micromechanical “drop-in” pattern, analogous to the set of test structures used in microelectronics for measuring transistor parameters, which can be used to monitor MEMS process uniformity and repeatability, and to determine the mechanical properties of micromechanical materials. The method used is called “M-Test”, in which the dependence of electrostatic pull-in voltage on device geometry is used as the primary measurement. Previously developed quantitative models for pull-in of highly ideal structures, of the kind that can be fabricated with wafer bonding methods, were reported by Osterberg. These models have been demonstrated as effective methods of material property measurement in devices that satisfy their geometric assumptions. These methods have now been quantitatively extended to structures with built up, somewhat compliant supports, and to materials, such as polysilicon, that exhibit residual strain and strain gradients through their thickness. The Gupta Ph.D. thesis documents these results in detail.

An important issue that has emerged from the M-Test work is the critical role of accurate device metrology (see Figure 8). The pull-in voltage is a strong function of both the free-space gap beneath the M-Test structures, and the structure’s thickness. We discovered that improved calibration standards were needed for our surface profilometry tools in order to reduce the absolute errors of material property extraction. Two-wavelength double-angle ellipsometry has been used to provide independent calibration of a set of etched calibration standards; these can now be used to calibrate the profilometer *in-situ* when making measurements of device gaps and thicknesses.

*continued*

## Long Term Stability of Polysilicon Micromechanical Structures

### Personnel

W. VanArsdell  
(H. L. Tuller in collaboration with S. Brown)

### Sponsorship

NSF

A related issue concerns cantilever curvature when the structural layer has a strain gradient. We have recently used the Wyko interference surface profilometer to improve the accuracy of the determination of the residual strain gradient. The fact that the pull-in voltage is quite sensitive to cantilever curvature, in turn, opens up a new research use for the M-Test concept. This is reported separately (see "Microelectromechanical (MEMS) Thin-Film Stress Sensors"). □

Failure modes and long term stability of polysilicon micromechanical structures (MEMS) are being studied. A MEMS test specimen capable of investigating cyclic fatigue has been designed as well as a technique for precracking fatigue specimens using a nanoindenter. Experiments have demonstrated that these structures are subject to time dependent subcritical crack growth. □

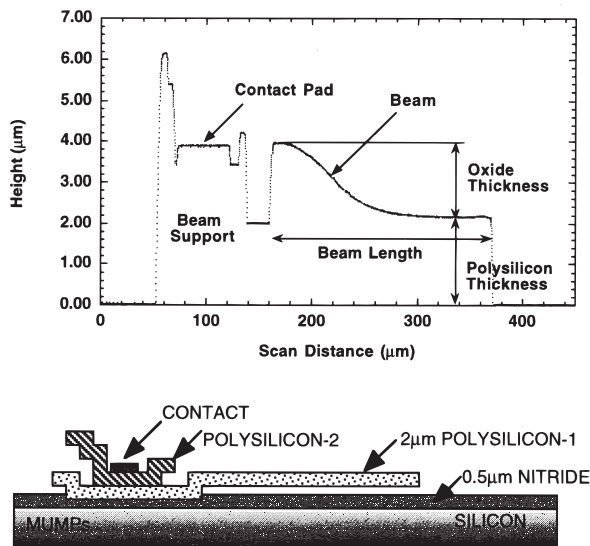


Fig. 8



---

## Microcantilever Beam Structures

---

### Personnel

Y. K. Min  
(H. L. Tuller)

### Sponsorship

Daewoo Electronics Fellowship

Silicon microcantilever beams, coated with piezoelectric films and a variety of other active materials will be examined for their response to a variety of thermal, chemical and mechanical stimuli. □

---

## Microelectromechanical Relays

---

### Personnel

J.-E. Wong  
(J. H. Lang and M. A. Schmidt)

### Sponsorship

CP Clare Corporation

This project continues to explore the application of silicon microfabrication technologies to the development of millimeter-scale relays. The relays under development are intended for use in controlling power, as opposed to switching signals. The potential advantages of these relays include low cost, small size, low power dissipation, and fast switching.

In addition to the development of millimeter-scale relays, this project studies the scientific phenomena of electrical breakdown across small air gaps, and the electrical and mechanical behavior of miniature relay contacts during closing, conduction, and opening. The results of this study will be used to guide the design of the relays. □

---

# CAD for Microelectromechanical Systems (MEMCAD)

---

## Personnel

L. Gabbay, V. Rabinovich, and B. Romanowicz  
(S. D. Senturia in collaboration with the research group of J. K. White and with Microcosm Technologies)

## Sponsorship

DARPA

The goal of this project has been to create a CAD system which is directed toward mechanical and electromechanical aspects of microsystem design. The MIT MEMCAD system has been licensed to Microcosm Technologies, Inc. for commercial distribution. Continuing work at MIT has focused on new classes of problems that will enhance the breadth of device applications for MEMCAD.

Perhaps the most critical need in such systems is the ability to construct low-order dynamic macro-models of device behavior that can be used in system-level simulators (such as SPICE), while maintaining consistency with the true behavior as represented by meshed simulation (see Figure 9). The TCAD portion of the MEMCAD system generates the device shape based on masks and process information, and the device simulators evaluate responses to applied loads in a highly meshed, numerically intensive environment. At the system level, however, where it is desirable to connect the MEMS device

into circuits, and to understand the effects of feedback, accurate and energetically correct low-order dynamical behavior models are needed, either in the form of equivalent lumped circuit models, or as a small number of coupled Ordinary Differential Equations (ODE's).

We have previously reported on use of basis-function methods for the construction of dynamic macro-models. In the original work, the nonlinear actuation forces were described only in direct space, not in basis-function coordinates. Now, we have developed an algorithmic procedure for automatically creating representations of electrostatic actuation and elastic behavior directly in

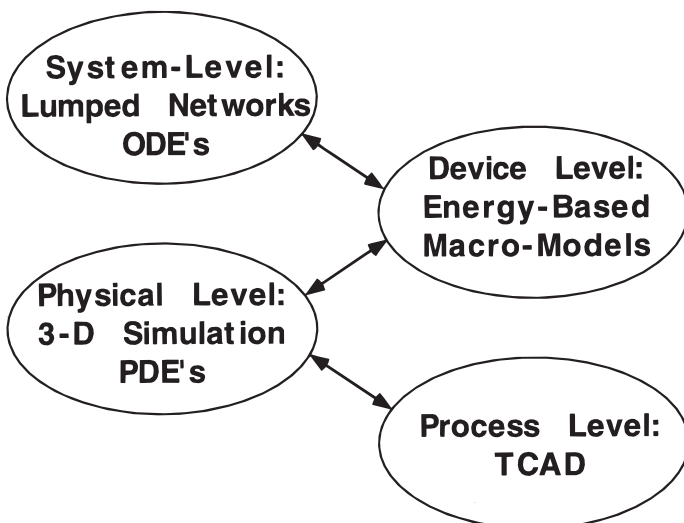


Fig. 9

Fig. 10

*continued*

basis-function space, leading to a small number of coupled ODE's that completely describe the device dynamics (but without damping) (see Figure 10). Further, the ODE's are written in a form which permits direct insertion into circuit simulators as a single function block, so that effects of an external circuit and feedback loop can be simulated.

Also, in previous work, we have demonstrated that the basis-function idea can be extended to systems with dissipation, provided one has access to an explicit-dynamics simulation for the coupled conservative and dissipative degrees of freedom (such as the air damping of a moving elastic body). We are now exploring whether it might be possible to use the automatically generated macro-model for the conservative part of the system to apply time-dependent boundary conditions to the dissipative (fluidic) part of the system, thereby greatly speeding up the total time required to generate a useful macro-model that includes dissipative effects. □

### Personnel

E. Peterson and J. Cottrell  
(M. B. McIlrath and D. E. Troxel)

### Sponsorship

DARPA and Stanford University

MEMS have the potential to revolutionize the design and production of sensors and actuators. However, the ultimate introduction of MEMS into major military and commercial systems depends critically on the speed with which MEMS can be designed and delivered into the field. The paucity of test equipment now available is an obstacle to the dissemination of MEMS for increasing the nation's defense and commercial competitiveness.

We call computer microvision the combination of light microscopy, video imaging, and machine vision. We are developing a series of MEMS stations to collect image data on various MEMS devices. The series of measurement stations will have a modular structure to enable the deployment of cost-effective measurement stations for the task at hand. A relatively more expensive MEMS station will have expanded specifications. Our ultimate goal is to develop computer microvision as a useful tool for the design and manufacture of MEMS - a tool that will enable the measurement of dynamical properties of the materials used to fabricate the MEMS device, as well as to characterize MEMS components used in larger systems.

Work has begun to construct a MEMS station consisting of a pc, camera, probe station (including a microscope), stimulus generator, and strobe pulse generator. This system will provide pictures in order to analyze a candidate MEMS device. Considerable work has been done on the development of a strobe pulse generator to trigger a flash tube which illuminates the image to be captured. A novel technique for the generation of these pulses via a software algorithm has been proposed and will be evaluated and compared to the traditional approach using a phase locked loop. □

# The Polychromator: A MEMS Correlation Spectrometer

## Personnel

E. Hung, E. Deutsch, and M. Hopgood  
(S. D. Senturia in collaboration with Honeywell Technology Center and Sandia National Laboratory)

## Sponsorship

DARPA

There are a number of promising applications for MEMS devices in the field of optics. This project explores a particular application in infrared spectroscopy. The basic concept is to use a linear array of mirrors, each one of which can be vertically positioned throughout a gap of several microns. By adjusting the relative positions of the mirrors, it is possible to create a special kind of diffraction grating such that incident light is diffracted into a selected viewing angle at multiple wavelengths (hence the name, "Polychromator"; see Figure 11). In particular, it is possible to create artificially the absorption or emission spectrum of a target molecule. Then, by modulating the lines in the target spectrum, one can build a new kind of correlation spectrometer – one which uses artificially created spectral features to correlate with the presence or absence of specific absorption lines in the incoming light. The Polychromator has many advantages over conventional correlation spectroscopy: (1) the Polychromator replaces the reference gas cell with a synthetic spectral device that can be programmed for many different species; (2) it is easy to

modulate compared to gas cells; (3) by using the emission spectrum instead of the gas-cell absorption for the correlation, the overall intensity is lowered, reducing detector shot noise; and (4) interferences between species can be omitted from the synthetic target spectrum by design.

The Polychromator is now being developed by a joint MIT-Honeywell-Sandia Labs team. The MIT part is the electromechanical design of the device, and the control algorithms. Since the device is fabricated with surface micromachining, which limits thicknesses of gaps to several microns, it is important to be able to achieve controllable travel across the full gap without encountering pull-in. A design that achieves this end, based on the principle of "leveraged bending" has been designed and tested (see Figure 12). Full Polychromator devices of 1024 lines are now in fabrication based on this pixel design. □

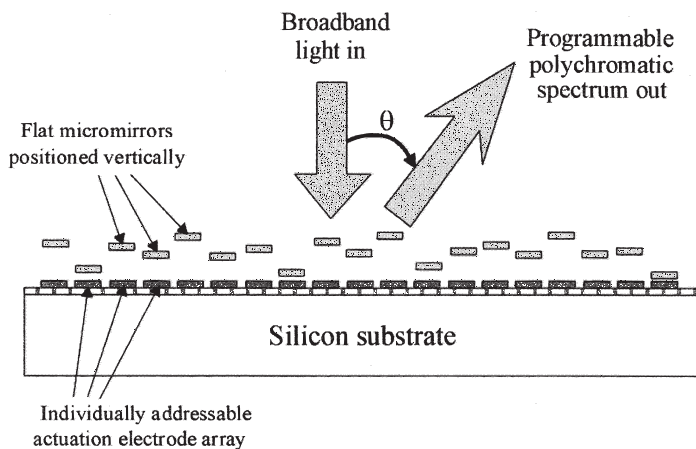


Fig. 11

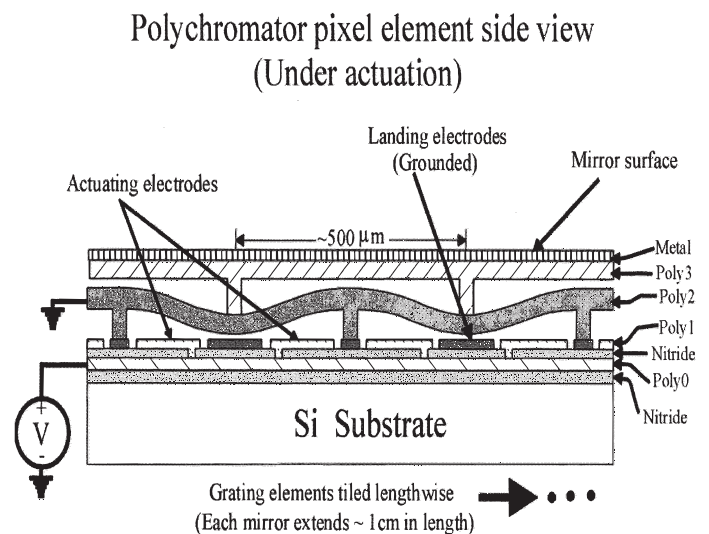


Fig. 12

# Aluminum Nitride for Bragg Reflector Thin-Film Resonators and Flexural Plate Wave Chemical Sensors

## Personnel

P. Hsieh and R. Naik  
(R. Reif)

## Sponsorship

SRC and Draper Laboratory

Low-temperature deposited AlN thin-films can be used in many novel, Si integrated devices such as RF Bandpass Filters and FPW Chemical Sensors. The modified Perkin-Elmer DC sputter deposition system in MTL has the capability to deposit 2.3° rocking curve AlN films on Si substrates at temperatures less than 200° C. Such high quality films can only be attained after rigorous minimization of the oxygen content. The film stress is usually highly tensile, in excess of 1 GPa for 0.5 μm thick AlN films. A significant stress reduction to approximately a few hundred MPa tensile was achieved by reconfiguring the gas flow, at the expense of an increase in the rocking curve to approximately 4°. It is expected that the film quality can be improved while maintaining the low stress once a design set of experiments is completed.

A Bragg Reflector TFR was fabricated at Lucent Technologies with AlN as the piezoelectric material and sputtered SiO<sub>2</sub> and AlNO<sub>x</sub> as the mirror materials. A  $k_{\text{eff}}^2$  of 3.6% corresponding to a TFR bandwidth of 22 MHz and a device  $Q$  of 400 rad. were measured at approximately 1.8 GHz. The low figures of merit are attributed to a poor acoustic mirror reflection coefficient. The poor reflection coefficient is due to variations of the mirror materials acoustic properties and thicknesses. If the acoustic properties of the mirror materials are well characterized, and the AlN piezoelectric film quality sufficiently high, substantially better figures of merit can be attained.

## Bragg Reflector TFR Fabrication

Figure 13 shows a SEM cross-section of a four-pair Bragg Reflector TFR fabricated at Lucent Technologies. Low-temperature sputtered SiO<sub>2</sub> and AlNO<sub>x</sub> were used as the low and high acoustic impedance mirror materials respectively. Based on stiffness and density values obtained from literature, the acoustic mirror materials thicknesses were predicted to be approximately 0.6 μm

for SiO<sub>2</sub> and 1.4 μm for AlNO<sub>x</sub>. The AlN thickness was predicted to be approximately 2.6 μm for resonance at 1.8 GHz. Figure 14 shows the measured response of the device.

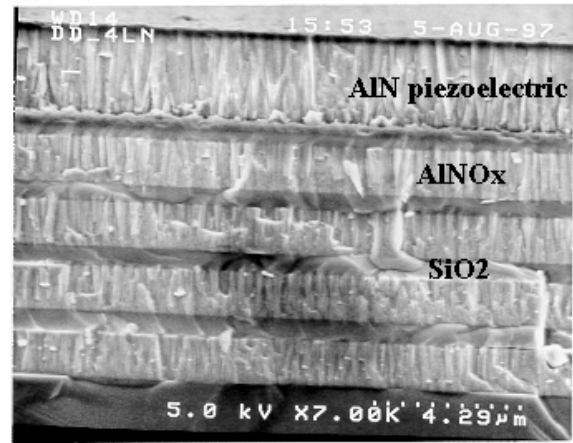


Fig. 13: SEM cross-section of a Bragg Reflector TFR. The top film is Al (invisible), followed by the AlN piezoelectric, followed by the bottom Al electrode (invisible), and then the four-pair acoustic mirror structure.

The resonance occurs at close to the targeted 1.8 GHz, therefore, this is an indication that the predicted, combined Al and AlN thicknesses and acoustic properties and the as-deposited thicknesses and acoustic properties are approximately equal. The bandwidth, insertion loss and device  $Q$  were measured to be 22 MHz, -3.2 dB and 400 rad. respectively.

The figures of merit for this device are low. In addition to the low figures of merit, periodic ripples can be observed within the main resonance. These ripples have a periodicity of approximately 6 MHz. The source of these ripples is standing waves which form within the bulk Si substrate. If the acoustic mirror is leaky, acoustic waves will penetrate the Si substrate, propagate within

*continued*

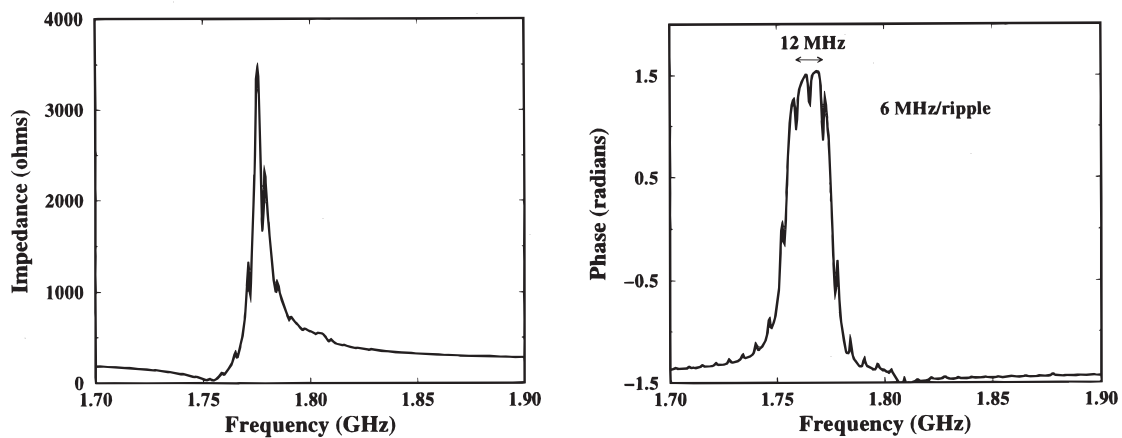


Fig. 14: Measured impedance response for a Bragg Reflector TFR device.

the substrate, reflect off the back-end and form standing waves within the entire structure. This hypothesis was confirmed by the fact that using Si substrates half as thick yielded a ripple spacing twice as large, and using Si substrates twice as thick yielded a ripple spacing half as large. The acoustic mirror is leaky for several reasons. Firstly, the as-deposited  $\text{SiO}_2$  and  $\text{AlNO}_x$  thicknesses are not exactly a quarter-wavelength. Secondly, the predicted stiffnesses and densities may not be the as-deposited stiffnesses and densities, in which case the impedance mismatch may be lower, and of course the as-deposited thicknesses will not be a quarter-wavelength.

The best solution is to measure the materials stiffnesses and densities accurately. Alternatively, the material velocities and densities can be measured, since the velocity is dependent on the stiffness and density. Once these acoustic properties are measured, it is essential from a manufacturing perspective that these properties are repeatable across the wafer, as well as from one wafer to the next. Another solution is to increase the

number of reflecting layer-pairs from four to five or perhaps six. However, not only will the fabrication time and cost increase, but the bandwidth will actually begin to decrease as acoustic energy is being stored in a much larger volume whenever more materials are added.

It is strongly expected that by measuring the materials acoustic properties, and depositing the correct thicknesses, the figures of merit can easily meet and exceed PCS specifications of a 30 MHz bandwidth and a  $Q$  of 1000.

One ultimate solution is to look for different acoustic mirror materials which have a higher impedance mismatch. In this case, the impact of variations in thickness, stiffness and density will be less severe. In addition, if the impedance mismatch is large enough, the number of reflecting layer pairs can be reduced from four to three or perhaps even two. The requirements for these new materials are that the measured impedance mismatch be greater than that of  $\text{SiO}_2$  and  $\text{AlNO}_x$ , that the quarter-wavelength thicknesses for these new

---

materials be reasonable, that these materials can be deposited quickly and stress-free, and that these materials are VLSI compatible.

### **Sputter Deposition for FPW Gravimetric Chemical Sensor**

0.5  $\mu\text{m}$  AlN films are deposited on Si membranes for use in FPW gravimetric sensors. Interdigitated transducers act on the piezoelectric AlN layer to launch and detect flexural plate waves across the membrane. The Si membranes are coated with binding-site specific polymers; exposure to target chemicals results in an increase in membrane mass. This mass change is detected as a change in the membrane FPW resonant frequency. Device sensitivity is dictated by membrane mass and hence the membrane thickness. Reduction in the AlN film thickness is desirable for increased device sensitivity.

Previously, film stress prove to be a significant factor in limiting further film thickness reduction. The 1 GPa tensile stress in the AlN layer caused severe deflection in the underlying membrane and raised concerns over device reliability. Gas flow reconfiguration has reduced film stress at the expense of film crystallinity and hence piezoelectric response. Further investigation with substrate heating seeks to improve film crystallinity while preserving low levels of AlN film stress. Characterization of the film morphology and materials properties is expected to lead to the identification of critical target deposition parameters for optimized film performance.  $\square$

---

## **Micromachined SIS Millimeter-Wave Focal-Plane Arrays**

---

### **Personnel**

G. de Lange, A. Rahman, E. Duerr, and K. Konistis (Q. Hu in collaboration with Dr. G. Sollner and Group 86 - MIT Lincoln Lab., Dr. A. Lichtenberger - Univ. of Va, and Dr. R. Robertazzi and Dr. D. Osterman - Hypres, Inc.)

### **Sponsorship**

NSF and NASA

SIS (superconductor-insulator-superconductor) heterodyne receivers have been demonstrated to be the most sensitive receivers throughout 30 - 840 GHz frequency range. The challenge now in the SIS receiver technology is to develop focal-plane arrays to improve the efficiency of data acquisition. In order to achieve these goals, we are currently developing a novel scheme to couple the millimeter-wave and infrared signals to the superconducting devices by using a micromachined horn antenna and a planar antenna supported by a thin ( $\sim 1 \mu\text{m}$ ) membrane, as shown in Figure 15(a). This novel micromachined antenna structure can be produced with a high precision using photolithography, and it can be utilized in focal-plane arrays, as shown in Figure 15(b).

Following our recent success in developing single-element micromachined SIS receivers (see our previous publication in *Appl. Phys. Lett.* **68**, 1862 (1996)), we have designed and constructed a  $3 \times 3$  focal-plane array with the center frequency around 200 GHz. The schematic of the structure is shown in Figure 16(a), which includes a micromachined and mechanically machined horn array, the device wafer, and the dc and IF connection board. Preliminary measurements of the dc I-V characteristics showed good uniformity across the entire array. Figure 16(b) shows the I-V curves from seven SIS junctions in the array. The resistance variation of these junctions is within 5%. Our heterodyne mixing measurement on a center element yielded a receiver noise as low as 50 K (DSB) at 190 GHz with a 3-dB bandwidth of 25 GHz. This result is comparable to the best achieved from conventional waveguide SIS receivers. We are currently in the process of measuring both the video and heterodyne response of the focal-plane array. Our next step will be to integrate on-chip Josephson-junction local oscillators with the SIS mixers to form monolithic focal-plane arrays.  $\square$

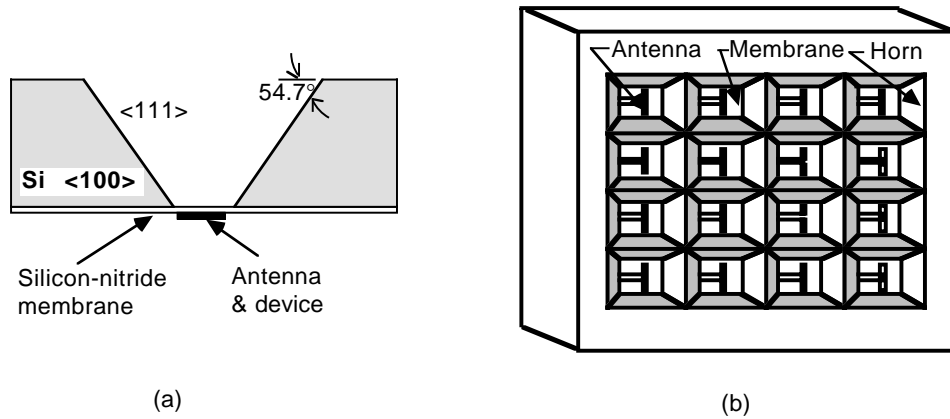


Fig. 15: (a) Example of a micromachined horn antenna structure that is made by anisotropically etching a <100> silicon wafer. (b) Schematic of a focal-plane array on a single wafer made using micromachining.

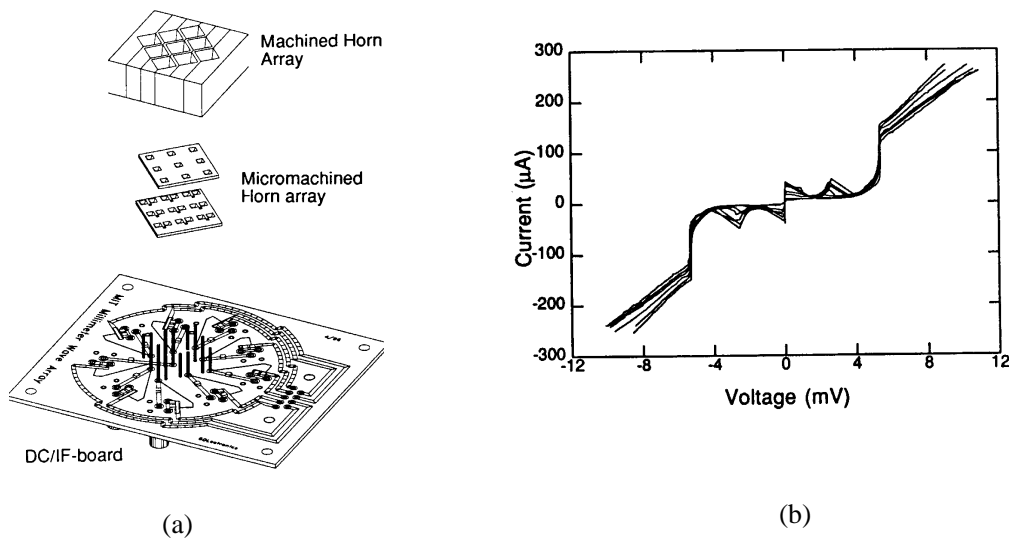


Fig. 16: (a) Schematic of an array structure including a micromachined and machined horn array, the device wafer, and the dc and IF connection board. (b) I-V curves of seven SIS junctions in the array.



---

# Micromachined Fluidic Systems for Biological Applications

---

## Personnel

J. Voldman and R. A. Braff  
(M. A. Schmidt, M. Gray, and M. Toner)

## Sponsorship

NSF

Many biological analysis instruments rely on the handling of small volumes of liquid, with and without biological cells. In this project, we have developed a mixing valve which is intended to mix two fluid streams under pressure, and achieve complete mixing in several seconds. A device has been microfabricated and tested.

The measurement results agree with model predictions. Figure 17 shows the schematic illustration of the mixer. More recently, we have begun to explore microfluidic systems which are specifically intended for manipulation and interrogation of biological cells. □

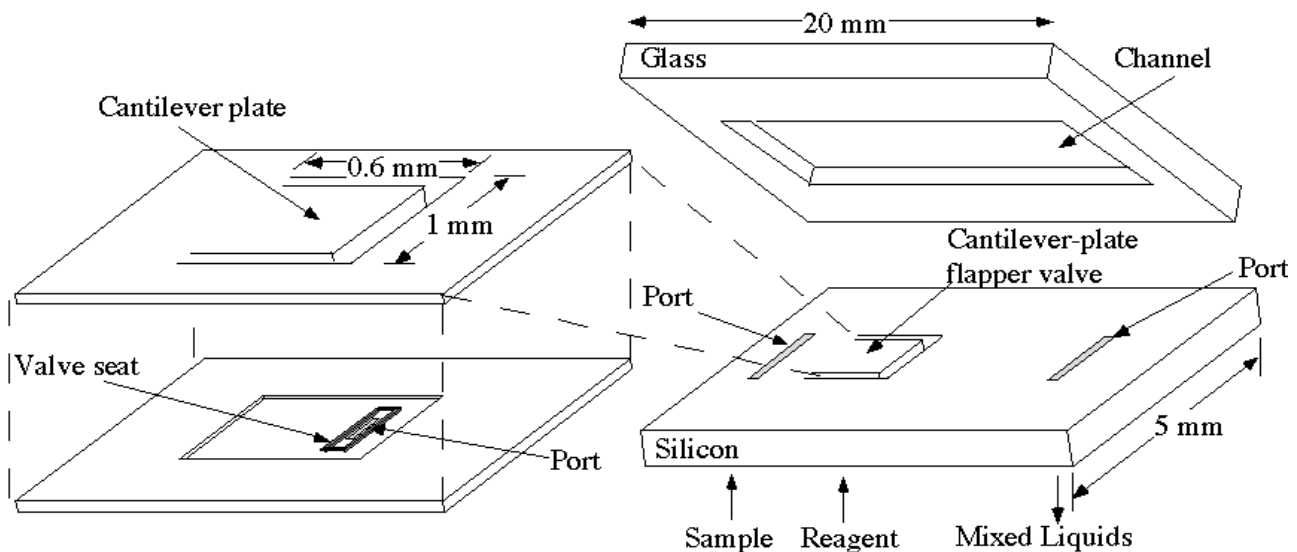


Fig. 17: A schematic illustration of a micromachined valve. (Courtesy of J. Voldman)

---

# Micromachined Chemical Reactors

---

## Personnel

S. Ajmera, S. Firebaugh, T. Floyd, A. Franz, M. Losey, D. Quiram, and T. Yu  
(M. A. Schmidt, M. J. Cima, and K. F. Jensen)

## Sponsorship

DARPA

Micromachined chemical systems have typically been fabricated for chemical analysis and sensing. Recently, reports have outlined the advantages of micromachined chemical systems for chemical production, and have demonstrated the feasibility of conducting reactions in externally heated microchannels. In this work, a  $\mu$ -reactor integrated with on-chip flow sensors, local heaters and temperature sensors is being fabricated, and tested by conducting a model catalytic oxidation reaction. The application for the  $\mu$ -reactor is chemical synthesis involving highly exothermic reactions. The large surface area to volume ratio facilitates very efficient heat removal, which prevents a thermal runaway, and inhibits undesired gas phase chemistry by thermal or chemical quenching of free radicals. Production of volumes of chemical would be achieved through the parallel connection of many reactors as shown in Figure 18. In addition, the  $\mu$ -reactor is a useful tool for fundamental reaction chemistry studies.

The project has activities in four major areas. First, we are studying gas phase reactions and methods of sensing these reactions. Second, we are developing robust reactors for elevated temperature using ceramic materials. Third, we are exploring technology for making liquid phase reactors. Finally, we are working in collaboration with DuPont corporation to demonstrate a scaled-up parallel reactor system.  $\square$

*Fig. 18: A parallel connection of many micromachined reactors.*

---

# Microelectromechanical (MEMS) Thin-Film Stress Sensors

---

## Personnel

A. Blanchet, E. Deutsch, S. Seel, and J. VanDeWeert  
(S. D. Senturia and C. Thompson)

## Sponsorship

DARPA, SRC, and NSF

We are developing the use of two types of MEMS devices for the measurement of stress in films during deposition and *in-situ* annealing. One class of devices uses micromachined single crystal microcantilevers with three resistors and one piezoresistor in a Wheatstone bridge fabricated in the cantilever. Piezoresistance measurements will be used to determine cantilever stresses resulting from stresses in films deposited on the cantilevers. The second class of devices is based on M-Test (see below). Both types of devices are being developed for *in-situ* mechanical analysis of films deposited in a wide variety of systems and conditions.

The M-Test concept (see “Microelectromechanical Test Structures (M-Test)”) offers an interesting opportunity to measure residual stress in extremely thin films. When a stressed thin film is deposited on a cantilever beam, the cantilever bends up or down depending on whether the thin film is in tensile or compressive stress, respectively. Because the pull-in voltage is directly dependent on the gap between the structure and the substrate, the stress-induced cantilever bending will modify the pull-in voltage. Hence, when supported by suitable models, the shift in pull-in voltage in combination with a knowledge of the deposited film thickness will permit *in-situ* extraction of the residual stress in very thin films, of order 100 Angstroms.

We are now working to develop these models and the associated measurement procedures. New 3-D MEMCAD simulations are being performed to account for the added cantilever curl that results from thin-film deposition. Data-reduction procedures are being tested to verify that extracted stress values are consistent across devices of varying geometries. In particular, direct optical measurement of cantilever curvature is being compared with pull-in shift, in order to assess quantitative accuracy and achievable error levels. Already, we have been able to demonstrate the pull-in shift due to a thin evaporated metal film on a silicon cantilever. The focus is now on documenting the quantitative integrity of the method, after which it will be applied to a variety of thin-film microelectronic materials. □

# Integrated Sensor Technology

## Personnel

C.-F. Yung, K. Ishihara, and C. Tsau  
(M. A. Schmidt)

## Sponsorship

DARPA and SRC

Much of the focus in the microsensor community today is in the direction of integration of sensors with electronics for signal-conditioning, communication and self-calibration/self-test. This program is investigating wafer-bonding and deep reactive ion etching technologies as a method of micromachining integrated sensors with integrated packaging. The device drivers for this project are an in-plane accelerometer, and a z-axis gyroscope (in collaboration with the University of California at Berkeley). The basic technology is illustrated in Figure 19. Wafer bonding is used to form a sealed cavity wafer which is compatible with IC processing at a foundry. This is followed by a deep reactive ion etch of the silicon to fashion the mechanical elements, and a low temperature bond which encapsulates the device and facilitates electrical lead-out. There are three short term goals for the program. The first is to fabricate an accelerometer with differential capacitive sensing and off-chip electronics which displaces in the plane of the wafer, as shown in Figure 20. The second is to fabricate a z-axis gyroscope through a collaborative program with the University of California at Berkeley and Honeywell.

The third is to establish the use of thermo-compression bonding as a means to accomplish wafer-level low temperature encapsulation of sensors in this process. The longer-term goals are to integrate CMOS electronics monolithically with the accelerometer and gyroscope, and to explore wafer-level vacuum sealing. □

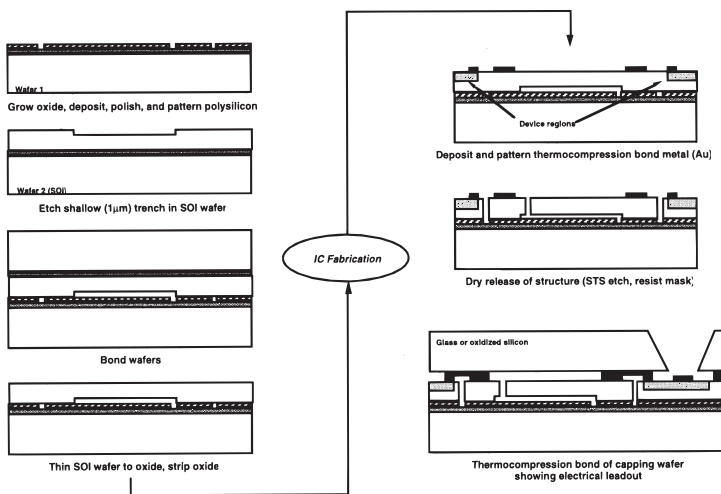


Fig. 20: SEM Photograph of a Lateral Capacitive Accelerometer (Courtesy of K. Ishihara).



Fig. 19: Demonstration of Integrated Sensor Process Flow.

---

# Silicon Sensors for the PHOBOS Experiment

---

## Personnel

G. van Nieuwenhuizen and S. G. Steadman

## Sponsorship

DOE/Brookhaven National Laboratory

PHOBOS is one of the four experiments being mounted at the new Relativistic Heavy Ion Collider at Brookhaven National Laboratory. In this collider gold ions will be accelerated to near light velocity and counter rotating beams will collide at four interaction regions. There the colliding ions will form matter with similar density and temperature as matter had a few seconds after the beginning of the universe. These densities and temperatures will be reflected by thousands of highly energetic particles coming out of these interactions. The four interaction regions are surrounded by particle detectors in order to characterize the reaction which took place. PHOBOS is one of these particle detectors and is built by several universities in the United States, Poland and Taiwan. The heavy-ion group of the Lab for Nuclear Science is the leading group in this collaboration.

The PHOBOS experiment will use 410 large area silicon sensors as particle detectors. Silicon sensors have outstanding characteristics when it comes to detecting fast particles. They can be made thin (300  $\mu\text{m}$ ) to reduce scattering and they have, when coupled to the proper electronics, an excellent signal-to-noise ratio. One sensor can be made almost as large as a four inch wafer and the sensor surface can be subdivided into pads, which makes for a large detection surface with high spatial resolution. The PHOBOS sensors are made as AC coupled, double-metal layer devices with a number of active pads anywhere between 128 and 1536. The first metal layer is needed to form coupling capacitors while the second metal layer is needed to form signal traces to feed the signals to the electronics mounted at the edge of the sensors. The silicon wafers used are high purity n-type silicon (5  $\text{k}\Omega\text{-cm}$ ) and the sensors will be reversed biased such that the whole 300  $\mu\text{m}$  depth will be fully depleted. Highly integrated electronics will be used to read out the sensors.

The silicon sensors are being produced by ERSO in Taiwan, supervised by the National Central University in Chung-Li. Until now 200 sensors have been received and are being tested at the sensor testing facility of the LNS heavy-ion group. In 1997 several batches of wafers were diced at MTL with different dicing parameters to study the influence of the cutting on the guard-ring leakage current. A single guard ring is used to maximize the active area and, for the same reason, the distance from guard to edge should be kept as small as possible. It was found that the minimum distance should be 300  $\mu\text{m}$ , otherwise the guard-ring leakage current will be excessive (more than 200  $\mu\text{A}$ ) at full depletion voltage.  $\square$

---

# Low Self-Noise Micromachined Microphones

---

## Personnel

M. Sheplak  
(M. A. Schmidt and K. S. Breuer)

## Sponsorship

NASA

Compliance with the FAR 36-Stage 3 community noise standard is one of the major factors determining the commercial viability of the High-Speed Civil Transport (HSCT). Noise generated during take-off and the approach are the primary aircraft operations determining airport noise levels. Data from forward-flight jet noise experiments plays an important role in verifying noise suppression techniques and guides the development of analytical models. Accurate simulation of these forward flight conditions requires that the acoustic measurements of the combustion system model be performed in a wind-tunnel. Unfortunately, the signal-to-noise ratio of conventional microphones is limited by the flow noise generated by the interaction of the microphone and the wind-tunnel flow. Nose cones reduce the level of this noise, but are subject to cavity- and boundary-layer noise. As a result, the overall noise floor of a conventional condenser microphone in this environment is unacceptably high. In fact, the noise floor is too high to permit complete characterization of the projected noise field radiated from a suppressed 1/7-scale HSCT nozzle meeting FAR 36-Stage 3. A microphone flush-mounted to the surface of a laminar-flow airfoil offers the potential to reduce wind noise to acceptable levels. Surface mounting requires that the side length of the microphone be much smaller than the local surface curvature. These constraints preclude the use of conventional condenser microphones. The primary goal of this research effort is to extend MEMS technology to the development of a low-noise, miniature microphone that can be flush-mounted on a laminar-flow airfoil.

A microphone is an electro-mechanical-acoustic transducer that transforms acoustical energy into electrical energy. Although many different transduction principles have been employed, all are based on the electronic measurement of a pressure-induced structural deflection. Most commercial microphones employ capacitive sensing schemes. The implementation of a capacitive scheme in solid-state sensors requires on-chip electronics to mini-

mize the effects of parasitic capacitance. The piezoresistive transduction scheme, which consists of measuring the strain on the top surface of a deflected diaphragm is less expensive to develop, simpler to fabricate, and potentially more robust than a capacitive device. These factors, along with concerns about environmental stability and first-run success lead to the selection of a piezoresistive sensing scheme for this project. The MIT microphone consists of a 1500Å, 210 μm diameter silicon-nitride membrane stretched over a circular cavity possessing, 850Å-thick, silicon-dioxide encapsulated, single-crystal silicon piezoresistors. The predicted resonant frequency of this device is 1.3 MHz. The winding vent channel provides the appropriate acoustic resistance for a 100 Hz low-frequency cut-off. A first-generation device has been successfully fabricated (see Figure 21) and is currently being tested. □

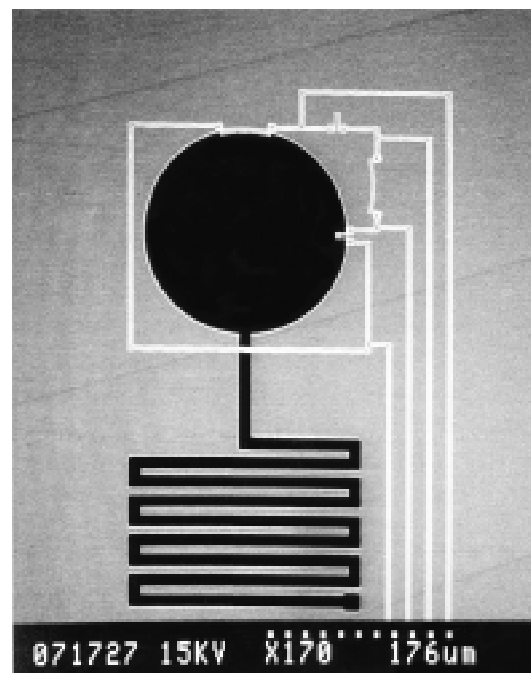


Fig. 21: SEM photo of a piezoresistive, circular-diaphragm microphone with a winding vent channel.